ORNL/SPR-2019/1146
Rev. 0

Methodology for Irradiation Creep Testing of SiC / SiC Composite Cladding

Nuclear Technology Research and Development

**Approved for public release.
Distribution is unlimited.**

Prepared for
U.S. Department of Energy
Nuclear Technology R&D
Advanced Fuels Campaign

Authors:
Patrick A. Champlin, Christian M. Petrie, and Kurt R. Smith
Oak Ridge National Laboratory

May 2019
ORNL/SPR-2019/1146

ACKNOWLEDGEMENTS

This research was sponsored by the Advanced Fuels Campaign (AFC) Program of the US Department of Energy (DOE), Office of Nuclear Energy. Neutron irradiation in the High Flux Isotope Reactor (HFIR) is made possible by the Office of Basic Energy Sciences, US DOE. The report was authored by UT-Battelle under Contract No. DE-AC05-00OR22725 with the US Department of Energy.

This page is intentionally left blank.

ABSTRACT

Irradiation creep compliance is a critical parameter for evaluating the stress evolution of silicon carbide (SiC) components during operation in various reactor concepts. Recent instrumented irradiation creep testing of SiC, performed at low dose in the Halden reactor, showed a creep compliance that is orders of magnitude higher than previous un-instrumented bend relaxation experiments performed in the High Flux Isotope Reactor (HFIR). This discrepancy illustrates the need for additional irradiation creep data for SiC. To this end, a novel irradiation capsule design has been developed to test miniature SiC tensile specimens under loading during irradiation in the HFIR. The experiment design uses the coolant pressure of the HFIR to compress a bellows, which applies the loading on the specimen. Preliminary thermal finite element models were developed to estimate the temperature distribution within the specimen and surrounding capsule components. Similar structural models were developed to evaluate the stress distribution within the specimen. The thermal analyses show that within the gauge section, the specimen temperatures remain within ~10°C of the nominal 300°C design temperature. Similarly, the structural analysis predicts axial stresses within ~10 MPa of the target stress of 100 MPa. These initial analyses show that irradiation creep testing of SiC in the HFIR is feasible and could provide a low-cost, high-throughput vehicle for gathering needed irradiation creep data.

This page is intentionally left blank.

CONTENTS

This page is intentionally left blank.

FIGURES

This page is intentionally left blank.

ACRONYMS

3D	three-dimensional
ANSYS	Analysis System Code
APDL	ANSYS Parametric Design Language
CAD	computer-aided design
CINDAS	Center for Information and Numerical Data Analysis and Synthesis
DAC	design and analysis calculation
HFIR	High Flux Isotope Reactor
MCNP	Monte Carlo N-Particle Code
ORNL	Oak Ridge National Laboratory
SiC	silicon carbide
TM	temperature monitor
VXF	Vertical Experiment Facility
TRRH	target rod rabbit holder

This page is intentionally left blank.

METHODOLOGY FOR IRRADIATION CREEP TESTING OF SIC/SIC COMPOSITE CLADDING

1. INTRODUCTION

Due to its resistance to high-temperature steam oxidation [1, 2], low neutron absorption, high-temperature strength retention, irradiation damage tolerance, and high melting point [3-5], silicon carbide (SiC) is being considered for use in a number of current and advanced reactor designs [6, 7]. While SiC has been shown to have large safety margins in accident scenarios [8], an improved understanding of thermomechanical properties is needed to validate steady-state models under normal operation [9, 10]. One critically lacking property is irradiation creep, which dictates the amount of deformation and stress relaxation at forces below the proportional limit stress, during irradiation. For both monolithic SiC (a brittle ceramic with a limited ability to accommodate strain) and SiC / SiC composites (continuous SiC fiber reinforced, SiC matrix composites with pseudo-ductility due to matrix micro-cracking and slip between the fibers and the matrix), understanding irradiation creep is essential to be able to accurately predict stress evolution resulting from a combination of the external coolant pressure, differential thermal/swelling strains, and pellet-cladding interactions [9, 11-13].

Previous experiments have attempted to measure irradiation creep in SiC under constant loading conditions using ion irradiation (highly accelerated damage rates) [14] and instrumented irradiation in the Halden reactor (low damage rates compared to typical light water reactors) [11]. One set of experiments performed in the High Flux Isotope Reactor (HFIR) used bend stress relaxation techniques to measure irradiation creep [12, 15, 16]. However, applied loading decreases over the course of the irradiation in such tests, which complicates the evaluation of irradiation creep compliance. Furthermore, non-uniformity in the specimen dimensions (particularly the thickness) can introduce significant error in the measurements. As such, irradiation creep data are very limited for homogeneous SiC and not currently available for SiC / SiC composites [17].

This report describes a versatile, low-cost irradiation creep experiment that can accommodate different sample materials, temperatures, and stresses. The design consists of a miniature tensile specimen loaded inside of a specialized rabbit housing that is seal-welded in an inert gas and irradiated in the flux trap of the HFIR. The HFIR coolant pressure is used to compress a small bellows that is welded to the rabbit housing, and this compression is used to apply a tensile load on the SiC specimen. More details regarding the capsule configuration and loading conditions are provided later in this report. The specimen stress is controlled by the diameter of the specimen, while temperature can be altered by modifying the size of an insulating gas gap inside the capsule. Because the HFIR coolant pressure remains constant throughout each irradiation cycle, the specimen loading should also remain constant. The cost of irradiating these specialized rabbit capsules would be comparable to that of other standard rabbit capsules, which would allow for evaluation of a large test matrix within a reasonable time and cost.

The experiment concept is similar to a previous design that used an internally pressurized bellows located inside a sealed rabbit housing. However, in that case, elevated temperatures are thought to have caused creep rupture of the bellows [18]. This issue is mitigated in the present design by putting the bellows in direct contact with the HFIR coolant. This report details the design of the SiC irradiation creep capsule, as well as initial thermal and structural finite element analyses to evaluate the distributions of temperature and stress in the specimens.

2. EXPERIMENT DESIGN CONCEPT

The rabbit capsules will be irradiated in the HFIR, which is a beryllium-reflected, pressurized, light water–cooled and moderated flux trap–type reactor [19]. The capsules will be loaded in a target rod rabbit holder (TRRH) position in the flux trap (the center of the reactor core). Because the HFIR operates continuously at a reactor power of 85 MW, the specimens will be exposed to a constant fast neutron flux of ~1×10^{15} n/cm^2/s. There are ~24 days in each HFIR cycle and the reactor coolant flows from top to bottom at a temperature in the range of 50−60°C.

Rabbit capsules are small, simple, cylindrical vessels that contain the specimens and the associated capsule components that hold the sample. The standard rabbit capsule design is modified for these experiments to include a bellows section. The experiment design concept is shown in Figure 1. The grip sections of a single SiC tensile specimen are pinned to the inner holder at one end and to the outer holder at the other end. The outer holder has a larger diameter than the inner holder, which allows the inner holder to pass freely inside of the outer holder. Both holders rest on ceramic blocks at the ends of the housing. A constant gas gap is maintained between the outer holder and the inner wall of the housing using tabs that are machined into the outer holder and a centering thimble located at the top of the outer holder. An insert is placed between the gauge section of the specimen and the inner holder to transfer heat from the specimen to the inner holder. The insert also holds a passive SiC temperature monitor (TM) that can be evaluated using dilatometry post-irradiation to estimate the temperature during irradiation [20], and swelling, which can be subtracted from the total expansion of the tensile specimen to quantify the expansion resulting only from irradiation creep.

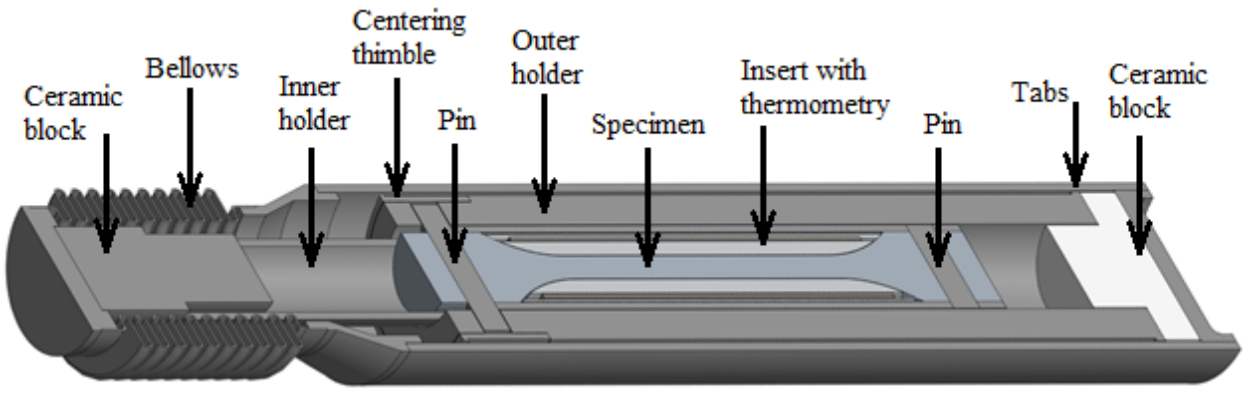

Figure 1. Design of the irradiation creep experiment.

The experiment components are contained within a specialized housing that incorporates a 10 mm-long bellows section that is welded to the top section of the housing while remaining within the envelope of a standard 64 mm long rabbit. Both the housing and the bellows are made of stainless steel in this case. The bellows compresses due to the pressure differential between the rabbit internals (~200 kPa) and the HFIR coolant (~3.2 MPa). The force that is exerted by the bellows compression is transmitted to the holders, moving the inner holder down and the outer holder up. As the inner holder is pulling down on the bottom of the specimen, and the outer holder is pulling up on the top of the specimen, this places the specimen in tension. The nominal specimen temperature and stress for these initial analyses are 300°C and 100 MPa, respectively. The gauge section of the specimen is 15 mm long, with an assumed diameter of 1.5 mm to achieve a 100 MPa loading. Overall, the specimen is 32 mm long.

3. COMPUTATIONAL METHODS

3.1 Thermal Analysis

To determine the three-dimensional (3D) temperature distribution in the assembly, the ANSYS finite element software is utilized with custom user-defined macros. One of these macros determines the thermal conductance between components separated by gas gaps that change due to thermal expansion [21]. This is calculated by applying a characteristic length *R* (e.g., the midpoint radius between the outer surface of the outer holder and the inner surface of the housing) to the following equation:

$$\delta_{hot} = \delta_{cold} + R \cdot [\alpha_t(T_t - T_{ref}) - \alpha_c(T_c - T_{ref})]$$

where:

δ_{hot} = effective separation distance between two contacting surfaces (m),
δ_{cold} = physical separation distance between two contacting surfaces at T_{ref} (m),
R = characteristic length for the contact-target combination
α_t, α_c = thermal expansion coefficients for the target and contact (m/m·K)
T_t, T_c = target and contact temperatures (°C),
T_{ref} = reference temperature for thermal expansion (°C),

This approach saves significant computation time by de-coupling the thermal and structural analyses, and by avoiding direct meshing of gas gaps. Derivation of this, and further detail for all ANSYS Parametric Design Language (APDL) macros used in the computation can be found in Design and Analysis Calculation (DAC) 11-13-ANSYS02, Rev. 6, which is available upon request [22]. The thermal analysis is performed after importing a computer aided design (CAD) model of the experiment into ANSYS and meshing the model with an element size ranging from 0.2-0.7 mm. Contacts are defined both to allow heat transfer between multiple bodies and to allow for structural interactions. Convection between the outer holder and the wall is assumed to be negligible, as there is little room for natural circulation to occur.

A database of DACs is maintained by the ORNL Nuclear Experiments and Irradiation Testing Group that includes the temperature-dependent thermophysical properties used in the analyses. Notably, the properties for SiC also include dose dependence. These properties are obtained from CINDAS [23], MatWeb [24], and various literature sources. The methods described by Wahid et al. are used to calculate the properties of gas mixtures [25]. Table 1 lists relevant DACs, which are available upon request.

Table 1. Experiment materials and material property references.

Part	Material	Reference
Specimen, thermometry	SiC	DAC-10-06-PROP_SIC(IRR) [26]
Inserts, holders, and specimen pins	Aluminum 6061	DAC-10-03-PROP_AL6061 [27]
Centering thimble	Ti-6Al-4V	DAC-11-14-PROP_TI6AL4V [28]
Ceramic blocks	Quartz	DAC-14-05-PROP_QUARTZ [29]
Housing, bellows, and rabbit end caps	Stainless steel 304L	DAC-10-16-PROP_SS304 [30]

Convection is applied to the outer surface of the rabbit housing, where convective heat transfer coefficients and bulk coolant temperatures are calculated using turbulent flow correlations and the axial power profile specific to the HFIR flux trap tube (from neutron and gamma heat generation in the coolant). Details of the

calculation can be found in DAC-11-01-RAB03 [31]. However, the temperature distribution of the rabbit internals is not particularly sensitive to these coefficients, with the housing surface typically being less than 10°C higher than the bulk coolant. Heat generation rates also vary as a function of axial position, with peak rates occurring at the reactor core midplane. Local heat generation rates can be estimated using the following profile:

$$q(\text{material}, z) = q_{peak}(\text{material}) \cdot \exp\left[-\left(\frac{z}{\sigma}\right)^2\right]$$

where:

q	=	local heat generation rate as a function of the material and axial location,
q_{peak}	=	heat generation rate at the HFIR midplane as a function of material,
z	=	axial location in the HFIR, where the midplane is at z = 0, and
σ	=	correlating parameter

These rates are calculated using the Monte Carlo N-Particle (MCNP) transport code, and they include contributions from prompt neutrons, prompt gamma photons, fission product decay photons, and decay (primarily due to beta emission) of activation sources. In this experiment, heating is dominated by gamma photon absorption. The peak heat generation rates, correlating parameter, and convection parameters are summarized in Table 2.

Table 2. Thermal boundary conditions.

Parameter	Value	Reference
Convective heat transfer coefficient	47.1 kW/m^2·K	DAC-11-01-RAB03 [31]
Bulk coolant temperature	52°C	DAC-11-01-RAB03 [31]
Correlating parameter	30.07 cm	C-HFIR-2012-035 Rev. 0 [32]
Peak heat generation rate for Al-6061	31.3 W/g	C-HFIR-2012-035 Rev. 0 [32]
Peak heat generation rate for SiC	31.7 W/g	C-HFIR-2012-035 Rev. 0 [32]
Peak heat generation rate for stainless steel*	38.1 W/g	C-HFIR-2012-035 Rev. 0 [32]
Peak heat generation rate for Ti-6Al-4V	35.2 W/g	C-HFIR-2013-003 Rev. 0 [33]
Peak heat generation rate for quartz	30.3 W/g	C-HFIR-2014-022 Rev. 0 [34]

*Originally evaluated for F82H stainless steel, where 304L is used here. This has negligible impact on the internal temperature profile as all steel is in contact with the coolant.

3.2 Structural Analysis

Following the thermal analysis, a simple structural analysis is performed on the ANSYS model described previously, using temperatures from the thermal calculation as input. Note that this is not a coupled-field approach where the thermal and structural solutions are solved simultaneously. Instead, the thermal and structural analyses are solved separately to save computational time. For these experiments, this is assumed to be sufficiently accurate as the two solutions should be independent after accounting for the effect of thermal expansion as detailed in Section 3.1. The structural analysis is conducted by applying a force equal to that expected from the bellows (~177 N) to the top of the housing with a fixed support boundary condition at the base. Material properties used for this analysis can be found in the DACs listed in Table 1.

4. ANALYSIS RESULTS

4.1 Thermal Analysis Results

The temperature profiles for the specimen and rabbit internals at the reactor midplane are presented in Figure 2. The temperature within the main body of the rabbit is relatively uniform due to the large amount of aluminum (with high thermal conductivity), the placement of the capsule near the reactor midplane (which reduces spatial gradients in heat generation), and the insulation provided by the ceramic blocks at each end of the capsule. The temperature of the gauge section of the specimen remains within 295−310°C, which is consistent with the target temperature of 300°C. This temperature can be modified by altering the fill gas and the size of the gas gap between the outer holder and the housing, where pure helium with a 0.23 mm gap is assumed to achieve design temperature. The specimen temperature near the top grip section is higher than the temperature near the bottom grip section primarily due to the much larger gas gap at the top of the experiment. The bellows remains relatively cool, with a temperature nearly equal to the temperature of the reactor coolant. This is important as high temperatures were identified to be problematic for bellows in previous experiments [18]. All temperatures in the rabbit remain well below the melting points of the respective materials under design conditions. Under a 130% reactor overpower, initial results predict a housing surface temperature of ~80°C and a maximum aluminum temperature of ~510°C. These values are lower for a 50% flow reduction.

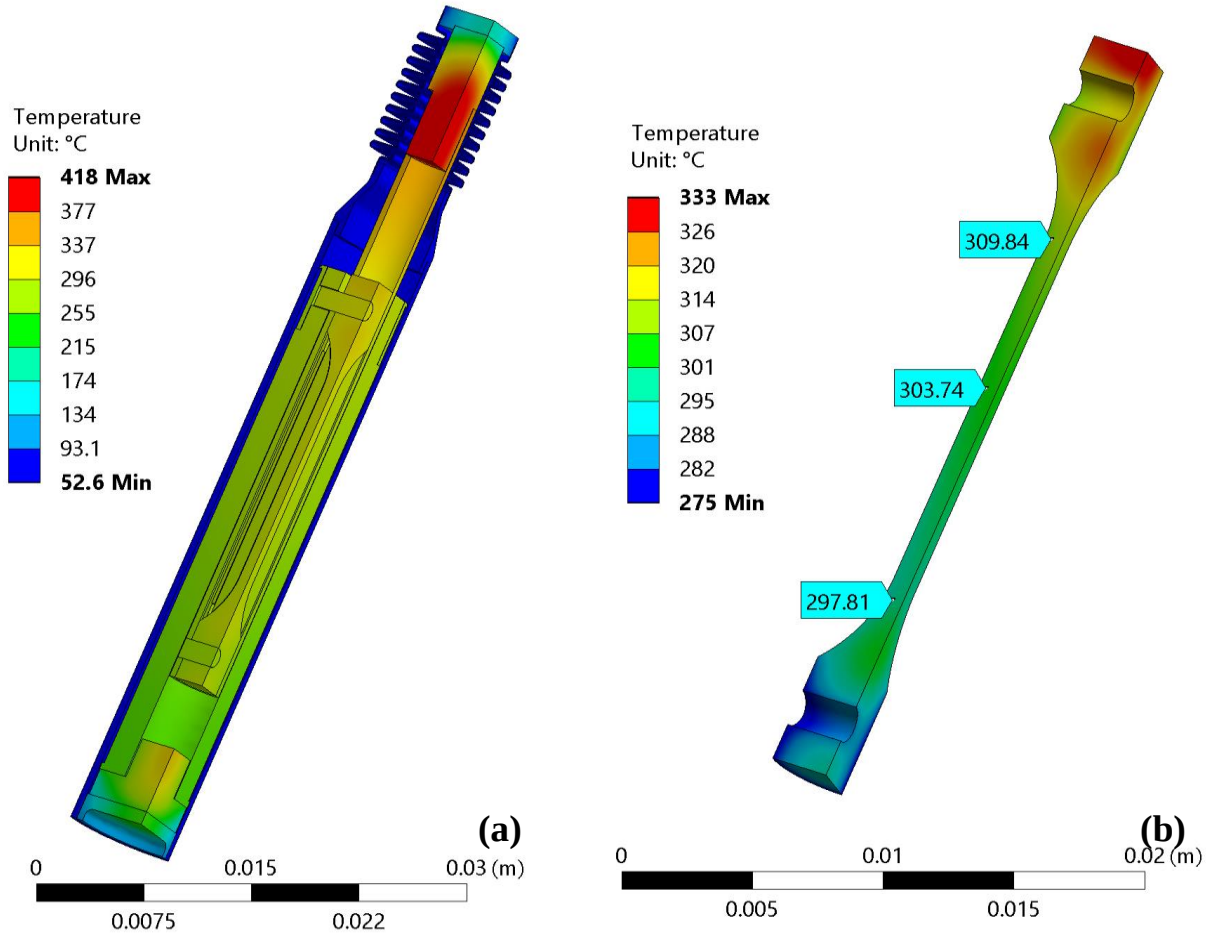

Figure 2. Predicted temperature contours for (a) the experiment assembly and (b) the SiC specimen.

4.2 Structural Analysis Results

Figure 3 shows the predicted axial stresses in the specimen, with values ranging from 100−110 MPa in the gauge section. Stresses increase near the pinned locations; however, the size of these concentrations shrink as the mesh is refined – indicating that they are highly localized. Future work will refine the stress calculations near the pin locations and modify the specimen geometry, if necessary, to ensure that the specimens will not fail near the pins. The experiment is designed so that the diameter of the specimen test region may be altered to achieve various levels of stress.

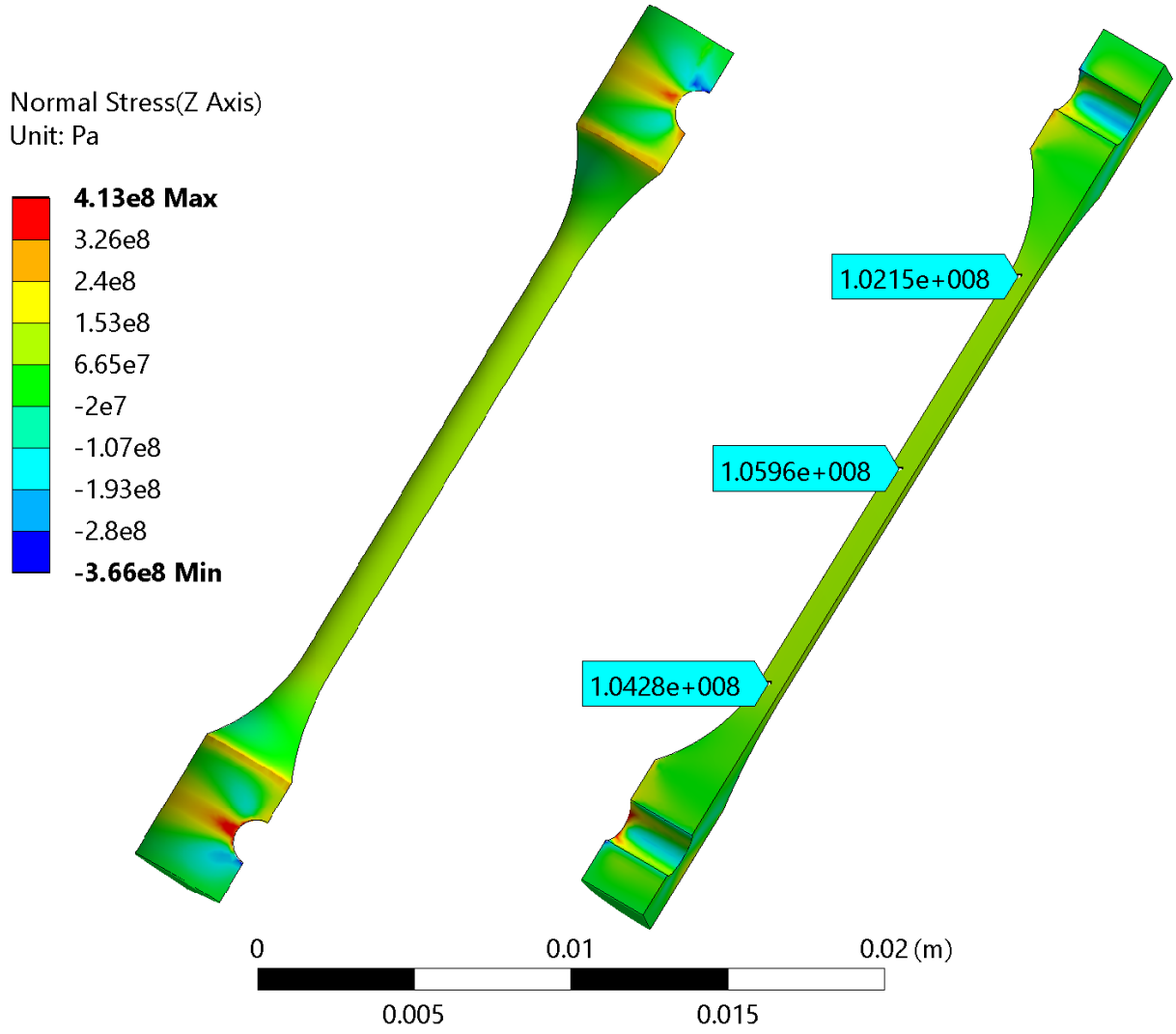

Figure 3. Predicted axial stress distribution in the specimen.

5. CONCLUSIONS AND FUTURE WORK

This report presents the design and initial analysis of a SiC creep capsule that will be irradiated in a TRRH position in the flux trap of the HFIR. The capsule was designed to irradiate a SiC specimen while under tensile loading from a pressurized bellows. The bellows is welded to the capsule housing, which is directly cooled by the HFIR coolant at 50−60°C. The HFIR coolant pressure causes the bellows to compress and provide a constant load on the SiC specimen during irradiation. This allows for highly-controlled irradiation conditions, which will provide simplified evaluations of irradiation creep compliance from the measured post-irradiation dimensional changes in the specimen.

The results of this experiment will be used to characterize irradiation creep in SiC, which is critical for accurate predictions of stress evolution in SiC components during operation in commercial reactors. As currently modeled, the temperature and tensile stress in the specimen gauge region are predicted to be within 295-310°C and 100-110 MPa, respectively. The specimen temperature is adjustable via the width of an insulating gas gap, and the stress can be varied by adjusting the diameter of the specimen gauge section. These initial analyses show that irradiation creep testing of SiC in the HFIR is feasible and could provide a low-cost, high-throughput vehicle for gathering critical irradiation creep data.

Future work will include physical testing, design iterations, and refinement of the numerical models. Prototype bellows will be investigated to ensure they can provide both the expected load and a sealed weld under design conditions. The specimen will be submitted to a standard tensile test before being used with the bellows and optimized for potential in-situ and post-irradiation load measurements. Finally, additional steps will be taken to verify that the design is acceptable under all possible safety-relevant conditions, expanding on those briefly presented in this report.

6. WORKS CITED

[1] Pint, B. A. et al., 2013, "High temperature Oxidation of Fuel Cladding Candidate Materials in Steam–hydrogen Environments," *Journal of Nuclear Materials*, **440** (1-3), pp. 420-427.

[2] Terrani, K. A. et al., 2014, "Silicon Carbide Oxidation in Steam up to 2 MPa," *Journal of the American Ceramic Society*, **97** (8), pp. 2331–2352.

[3] Katoh, Y. et al., 2012, "Radiation Effects in SiC for Nuclear Structural Applications," *Curr Opin Solid St M*, **16** (3), pp. 143-152.

[4] Katoh, Y. et al., 2014, "Current Status and Recent Research Achievements in SiC/SiC Composites," *Journal of Nuclear Materials*, **455** (1–3), pp. 387–397.

[5] Koyanagi, T., 2014, "Effects of Neutron Irradiation on Mechanical Properties of Silicon Carbide Composites Fabricated by Nano-infiltration and Transient Eutectic-phase Process," *Journal of Nuclear Materials*, **448**, pp. 478-486.

[6] Deck, C. P. et al., 2015, "Characterization of SiC–SiC Composites for Accident Tolerant Fuel Cladding," *Journal of Nuclear Materials*, **466**, pp. 667–681.

[7] Snead, L. L. et al., 2011, "Silicon Carbide Composites as Fusion Power Reactor Structural Materials," *Journal of Nuclear Materials*, **417** (1-3), pp. 330-339.

[8] Merrill, B. J. and Bragg-Sitton, S. M., 2013, "SiC Modifications to MELCOR for Severe Accident Analysis Applications," INL/CON-13-29076, 2013 LWR Fuel Performance Meeting / Top Fuel, Charlotte, NC.

[9] Ben-Belgacem, M. et al., 2014, "Thermo-mechanical Analysis of LWR SiC/SiC Composite Cladding," *Journal of Nuclear Materials*, **447** (1–3), pp. 125–142.

[10] Lee, Y. and Kazimi, M. S., 2015, "A Structural Model for Multi-layered Ceramic Cylinders and its Application to Silicon Carbide Cladding of Light Water Reactor Fuel," *Journal of Nuclear Materials*, **458**, pp. 87–105.

[11] Terrani, K. A., Karlsen, T.M., and Yamamoto, Y., 2016, "Input Correlations for Irradiation Creep of FeCrAl and SiC Based on In-Pile Halden Test Results," ORNL/TM-2016/191, Oak Ridge National Laboratory, Oak Ridge, TN.

[12] Koyanagi, T. et al., 2016, "Neutron-irradiation Creep of Silicon Carbide Materials Beyond the Initial Transient," *Journal of Nuclear Materials*, **478**, pp. 97-111.

[13] Petrie, C. M. et al., 2017, "Experimental Design and Analysis for Irradiation of SiC/SiC Composite Tubes under a Prototypic High Heat Flux," *J. Nucl. Mater.*, **491**.

[14] Kondo, S., Koyanagi, T., and Hinoki, T., 2014, "Irradiation Creep of 3C-SiC and Microstructural Understanding of the Underlying Mechanisms," *Journal of Nuclear Materials*, **448** (1-3), pp. 487-496.

[15] Morscher, G. N. and Dicarlo, J. A., 1992, "A Simple Test for Thermomechanical Evaluation of Ceramic Fibers," *Journal of the American Ceramic Society*, **75** (1), pp. 136-140.

[16] Katoh, Y. et al., 2013, "Observation and Possible Mechanism of Irradiation Induced Creep in Ceramics," *Journal of Nuclear Materials*, **434** (1), pp. 141–151.

[17] Koyanagi, T. et al., 2018, "Handbook of LWR SiC/SiC Cladding Properties - Revision 1," ORNL/TM-2018/912, Oak Ridge National Laboratory, Oak Ridge, TN. Available: https://www.osti.gov/servlets/purl/1479750.

[18] Byun, T. S. et al., 2013, "Principles and Practice of a Bellows-loaded Compact Irradiation Vehicle," *Journal of Nuclear Materials*, **439** (1-3), pp. 108-116.

[19] Xoubi, N. and Primm, R. T., 2005, "Modeling of the High Flux Isotope Reactor Cycle 400," ORNL/TM-2004/251, Oak Ridge, TN.

[20] Field, K. G. et al., 2019, "Evaluation of the Continuous Dilatometer Method of Silicon Carbide Thermometry for Passive Irradiation Temperature Determination," *Nuclear Instruments and Methods in Physics Research Section B: Beam Interactions with Materials and Atoms*, **445**, pp. 46-56.

[21] McDuffee, J. L., 2013, "Heat Transfer through Small Moveable Gas Gaps in M multi-body System using the ANSYS Finite Element Software," *ASME Summer Heat Transfer Conference*, Minneapolis, MN, United States.

[22] McDuffee, J. L., 2016, "Solve Macros for ANSYS Finite Element Models With Contact Elements," DAC-11-13-ANSYS02, Rev. 6, Oak Ridge National Laboratory, Oak Ridge, TN.

[23] *CINDAS, LLC: Global Benchmark for Critically Evaluated Materials Properties Data*, [cited 2016 27 July]. Available from: http://cindasdata.com.

[24] *MatWeb: Material Property Data*, [cited 2016 27 July]. Available from: http://matweb.com/.

[25] Wahid, S. M. S. and Madhusudana, C.V., 2000, "Gap conductance in contact heat transfer," *International Journal of Heat and Mass Transfer*, **43**, pp. 4483-4487.

[26] McDuffee, J. L., 2013, "Thermophysical Properties for Irradiated SiC," DAC-10-06-PROP_SIC(IRR), Rev. 3, Oak Ridge National Laboratory, Oak Ridge, TN.

[27] McDuffee, J. L., 2013, "Thermophysical Properties for AL6061," DAC-10-03-PROP_AL6061, Rev. 2, Oak Ridge National Laboratory, Oak Ridge, TN.

[28] McDuffee, J. L., 2013, "Thermophysical Properties for Titanium Alloy Ti-6Al4V," DAC-11-14-PROP_TI6AL4V, Rev. 1, Oak Ridge National Laboratory, Oak Ridge, TN.

[29] McDuffee, J. L., 2014, "Thermophysical Properties for Fused Silica Quartz," DAC-14-05-PROP_QUARTZ, Rev.0, Oak Ridge National Laboratory, Oak Ridge, TN.

[30] McDuffee, J. L., 2010, "Thermophysical Properties for 304 Stainless Steel," DAC-10-16-PROP_SS304 Rev. 0, Oak Ridge National Laboratory, Oak Ridge, TN.

[31] McDuffee, J. L., 2011, "Heat Transfer Coefficients and Bulk Temperatures for HFIR Rabbit Facilities," DAC-11-01-RAB03, Rev. 0, Oak Ridge National Laboratory, Oak Ridge, TN.

[32] McDuffee, J. L., 2012, "Heat Generation Rates for Various Rabbit Materials in the Flux Trap of HFIR," C-HFIR-2012-035, Rev. 0, Oak Ridge National Laboratory, Oak Ridge, TN.

[33] Daily, C. R., 2013, "Heat Generation Rates for Various Titanium and Silicon Compounds in the Flux Trap of HFIR," C-HFIR-2013-003, Rev. 0, Oak Ridge National Laboratory, Oak Ridge, TN.

[34] Daily, C. R., 2014, "Heat Generation Rates for Several Aluminum, Silicon, Titanium, Zirconium, Yttrium, and Tungsten Compounds to be Irradiated in the HFIR Flux Trap," C-HFIR-2014-022 Rev. 0, Oak Ridge National Laboratory, Oak Ridge, TN.